

# CHARACTERIZATION OF A FERROFLUID BY ATOMIC FORCE MICROSCOPY AND PHOTON CORRELATION SPECTROSCOPY AFTER MAGNETIC FRACTIONATION

C. Groß<sup>1</sup>, K. Büscher<sup>2</sup>, E. Romanus<sup>1</sup>, C.A. Helm<sup>2</sup> & W. Weitschies<sup>1</sup>

<sup>1</sup>[Institute of Pharmacy](#), University of Greifswald, Jahnstr. 17, D-17487 Greifswald, Germany

<sup>2</sup>[Institute of Applied Physics](#), University of Greifswald, Jahnstr. 16, D-17487 Greifswald, Germany

**INTRODUCTION:** Ferrofluids are colloidal solutions of magnetic nanoparticles in a carrier fluid. The nanoparticles consist of a ferri- or ferromagnetic core that is stabilized against aggregation by a shell based on various materials such as citrate ions or fatty acids. Ferrofluids are increasingly used for biological and medical applications, such as high gradient magnetic separation techniques [1], magnetic drug targeting [2], magnetic hyperthermia [3], contrast agents for Magnetic Resonance Imaging [4] and measurement of the relaxation of magnetic nanoparticles [5]. In all of these medical and biological applications the carrier fluid is water-based, while iron oxides (magnetite or maghemite) are predominantly chosen as core materials due to their proven biodegradability and low toxicity [6]. In order to avoid aggregation under physiological conditions (i.e., physiological pH values and salt concentrations), the nanosized magnetic cores are usually stabilized by shells derived from biocompatible polymeric carbohydrates such as dextrans or starch [7, 8].

In technical applications, concentrated ferrofluids are commonly used to obtain a “fluid magnet” with strong bulk magnetic properties, e.g. a high saturation magnetization. In contrast, in most medical and biological applications, the bulk magnetism of the ferrofluid is only of minor importance. Here, the properties of the individual nanoparticles contained in the fluid are more relevant. These properties include a high relaxation signal for nanoparticles used as contrast agents and a high magnetic moment for nanoparticles used as drug carriers in magnetic targeting or as separation devices in high gradient magnetic separation techniques.

It is well known, that the nanoparticles in ferrofluids produced by classical chemical syntheses display a rather broad particle size distribution [9]. This size distribution may either be due to variations of the core size, the thickness of the coating, or different stages of agglomeration (Fig. 1). In principle, the size of the magnetic cores can differ, whilst the thickness of the stabilizing coating remains constant (Fig. 1a) or is also variable (Fig. 1b). Furthermore, the size of the

magnetic cores may be rather constant, but some of the individual nanoparticles agglomerated during the synthesis, resulting in stable agglomerates with constant (Fig. 1c) or variable (Fig. 1d) thickness of the polymeric coating. Thirdly, the particle sizes may also vary due to the agglomeration of coated nanoparticles during storage (Fig. 1e, 1f).

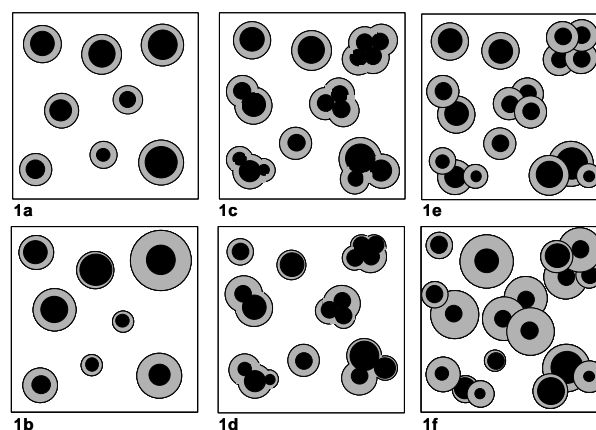


Fig. 1: Models for the origin of the nanoparticle size distribution in ferrofluids.

It was the aim of this study to investigate the size distribution of the magnetic nanoparticles in a water-based ferrofluid. For this purpose, a magnetic fractionation was performed and the fractions were characterized by atomic force microscopy (AFM) and photon correlation spectroscopy (PCS).

**MATERIALS & METHODS:** A water based ferrofluid (DDM 128N, Meito Sangyo, Japan) consisting of magnetic nanoparticles with a core of iron oxide and a shell of carboxydextran ( $M_r$  about 2000) were magnetically fractionated by stepwise reduction of the electromagnetic field from 6 A (1 T) to zero field using an electromagnet (Bruker B-MN 90/30) and magnetic separation columns (MACS Cell Separation Column LS, Miltenyi Biotec). A detailed description of the fractionation procedure is given elsewhere [9]. In brief, the separation columns were fixed between the pole shoes of the electromagnet and rinsed with 2 ml of buffer solution (phosphate buffered saline, pH 7.4). Then, at the highest current (6 A), 500  $\mu$ l of the ferrofluid was added. The column was rinsed with the buffer solution until the eluate was clear (6 A

fraction). Then the field was reduced and the next eluate was gathered. This procedure was repeated until zero current was applied. Then, the column was removed from the magnet and the remaining nanoparticles were eluated with buffer solution and gathered (fraction “out of magnet”).

The iron content of each fraction was determined by chemical analysis [10]. The hydrodynamic diameter of the nanoparticles was measured by PCS (ZetaSizer 3000HS, Malvern). Furthermore, fractions were also investigated by AFM in the tapping mode (Multimode-AFM with Nanoscope IIIa-controller, Digital Instruments) after electrostatic adsorption of the nanoparticles onto polyetheleneimine modified mica [11]. The particle diameters were determined from the height images. Furthermore the magnetic relaxation signals of the freeze dried fractions were measured at room temperature using a LTS SQUID gradiometer system described elsewhere [12] and calculated as magnetic relaxation signal (in pT) per molar content of iron (in  $\mu\text{mol}$ ) in the fractions.

**RESULTS:** The hydrodynamic diameters of the different fractions and the original ferrofluid as well as the particle diameters determined by AFM are given in Table 1.

*Table 1: Mean particle diameters of magnetically fractionated nanoparticles measured by PCS and AFM and the magnetic nanoparticle relaxation signal.*

Fraction	AFM (nm)	PCS (nm)	Magnetic relaxation signal (pT/ $\mu\text{mol}$ Fe)
Original	20	61	15
4 A	6	14	0
1 A	7	15	0
0.25 A	10	22	0
0.125 A	10	29	0
0.06 A	13	36	9
0.015 A	13	44	58
0 A	24	46	79
Out of magnet	29	66	167

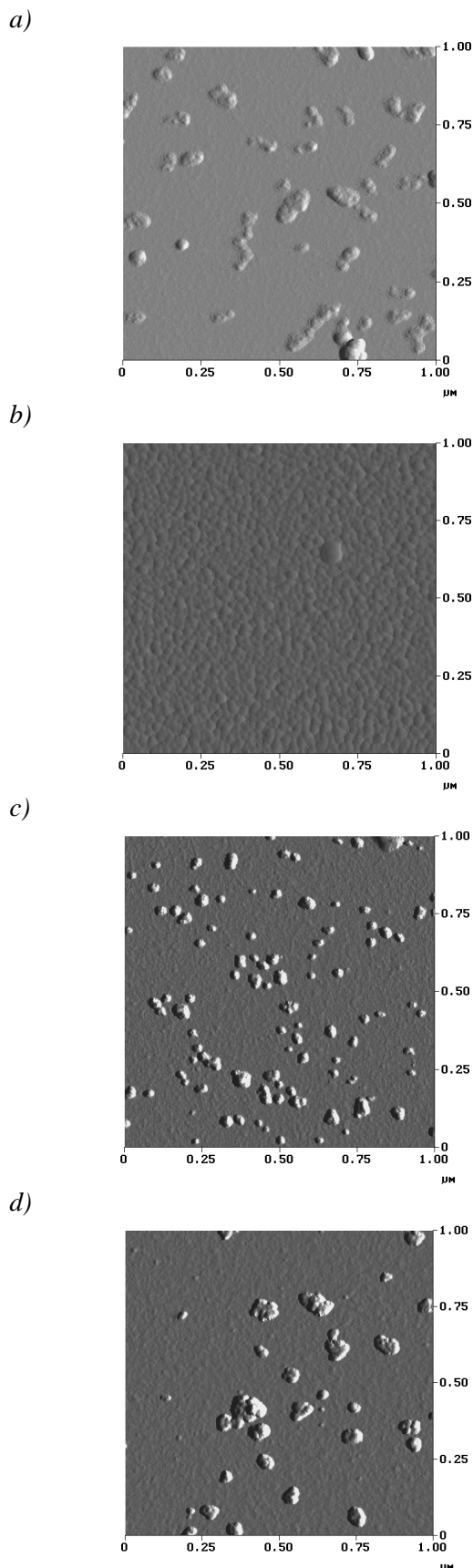


*Fig. 2: AFM-amplitude images of the (a) original ferrofluid, and the fractions gathered at (b) 4 A, (c) 0.125 A and (d) 0 A. The surface coverage is diffusion controlled.*

The fraction gathered at 6 A could not be evaluated by PCS, as the count rate was below the critical limit, indicating a very small particle size, that is mostly due to dissolved carboxydextran. The mean particle sizes as determined by PCS increase continuously from the fractions gathered at 4 A to the fraction that was finally rinsed after removal of the column from the magnet (fraction: “out of magnet”). This increase in the mean particle diameters could also be observed by AFM.

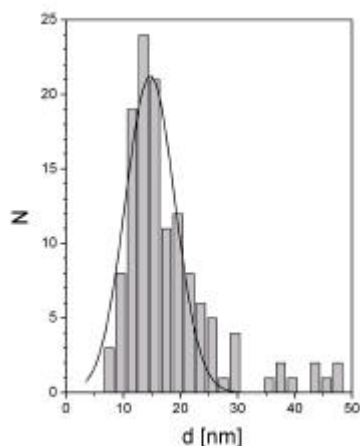


Fig. 3: Histogram of the particle size distribution of the original ferrofluid before fractionation as determined from the AFM-amplitude image with overlaid Gauss curve.

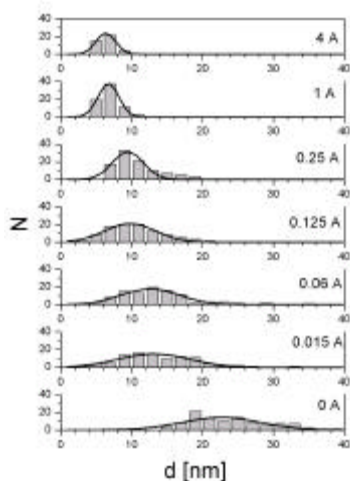


Fig. 4: Histograms of the particle size distributions of fractions of a ferrofluid as determined from AFM-amplitude images.

A magnetic nanoparticle relaxation signal could only be found for the fractions gathered below 0.125 A, whilst the strength of the magnetic signal increases with decreasing current and increasing particle size.

In the AFM-amplitude image of the original ferrofluid before fractionation (Fig. 2a) single nanoparticles and agglomerates are present. The nanoparticles gathered at 4 A are free of agglomerates (Fig. 2b). They form an adsorption layer on the mica surface. In contrast, the fractions gathered at lower currents (Fig. 2c and 2d) are predominantly formed by agglomerates with increasing diameters. The histograms of the particle size distributions of the original ferrofluid (Fig. 3) and the fractions (Fig. 4) show, that the particle size distribution broadens with increasing particle size.

**DISCUSSION & CONCLUSIONS:** During magnetic fractionation the magnetic nanoparticles are separated according to their magnetic moments. As the magnetic moment of a single domain magnetic nanoparticle is proportional to the amount of magnetic material, i.e. the volume of the magnetic core, only particles with very small core sizes pass the column at high magnetic field strengths, i.e. high applied currents. This could be confirmed by the AFM and the PCS measurements. The immeasurable signal in the magnetic nanoparticle relaxation measurements reconfirms this result, as the magnetic relaxation signal of single domain particles is also strongly dependent on the particle size [13].

The AFM images show, that the larger nanoparticles are mostly agglomerates of small nanoparticles. It can be ruled out, that these agglomerates had been formed during the fractionation process or that they are artifacts derived from the preparation of the AFM samples, as the mean hydrodynamic diameter of the reunified fractions was found to be nearly identical to the mean hydrodynamic particle diameter determined before fractionation (65 nm versus 61 nm).

The magnetic relaxation signals measured for fractions gathered at low currents indicate, that some nanoparticles with relatively large core diameters are also present, but they are only representing a minor proportion.

The comparison of the mean particle sizes determined by AFM and PCS further indicates, that the mean diameters yielded by PCS measurements are mostly determined by large particles that are present in the sample. This is due to the fact that the PCS signal derived from nanoparticles with diameters far below the laser wavelength (in our case 630 nm) is dominated by Rayleigh diffraction. In Rayleigh diffraction, the intensity of the signal depends on the diameter of the particle, specifically the diameter raised to the power of six.

With respect to the different models presented for the origin of particle size distributions in Fig. 1, we conclude, that the investigated ferrofluid will most probably be described by Fig. 1c, although the model in Fig. 1d cannot be ruled out entirely.

Knowledge about the inner structure of magnetic nanoparticles with larger diameters may have great implications for their biological or medical applications. This can be explained with the following example: Two magnetic nanoparticles with identical particle diameters consist either of an agglomerate of a number of small magnetic cores or one single magnetic core. Assuming that the magnetic particles will not interfere magnetically without the presence of an external magnetic field, the magnetic moment of the agglomerate will be low or even zero in the absence of an external magnetizing field, as the magnetic moments of the individual cores will be statistically distributed. In the presence of an external field, the directions of the magnetic moments will align in the direction of this field and generate a strong magnetic moment. In contrast, the strength of the magnetic moment of the nanoparticle composed of one magnetic core will be independent of the external magnetic field, only its orientation will be influenced by the external field. Therefore, in applications where no or only weak external magnetic fields will be applied, the nanoparticle composed of several magnetic cores will not provide a magnetic force, whilst in applications where strong magnetic fields are applied, the two nanoparticles will yield comparable magnetic forces. In order to use magnetic nanoparticles in biological or medical applications it is therefore important to know which properties of magnetic nanoparticles are needed and which kind of nanoparticles are really present in the ferrofluid.

**REFERENCES:** <sup>1</sup>A. Radbruch, B. Mechtold, A. Thiel, S. Miltenyi and E. Pfluger (1994) *High-gradient magnetic cell sorting* Methods Cell Biol **42**: 387 <sup>2</sup>A.S. Lübbe, C. Alexiou and C. Bergemann (2001) *Clinical applications of magnetic drug targeting* J Surg Res **95**: 200-206 <sup>3</sup>A. Jordan, P. Wust, H. Fähling, W. John, A. Hinz and R. Felix (1993) *Inductive heating of ferrimagnetic particles and magnetic fluids: physical evaluation of their potential of hyperthermia* Int. J. Hyperthermia **9**: 51-68 <sup>4</sup>D. Pouliquen, H. Perroud, F. Calza, P. Jallet and J.J. Le Jeune (1992) *Investigation of the magnetic properties of iron oxide nanoparticles used as contrast agent for MRI* Magn. Reson. Med. **24**: 75-84 <sup>5</sup>W. Weitschies, R. Kötz, T. Bunte and L.

Trahms (1997) *Determination of relaxing or remanent nanoparticle magnetization provides a novel binding specific technique for the evaluation of immunosassays* Pharm. Pharmacol. Lett. **7**: 5-8 <sup>6</sup>F. Kopp, M. Laniado, F. Dammann, F. Stern, E. Gronewaller, T. Balzer, C. Schimpfky and C.D. Claussen (1997) *MR imaging of the liver with Resovist: safety, efficacy and pharmacodynamic properties* Radiology **204**: 749-756 <sup>7</sup>L.M. Lacava, Z.G. Lacava, M.F. Da Silva, O. Silva, S.B. Chaves, R.B. Azevedo, F. Pelegrini, C. Gansau, N. Buske, D. Sabolovic and P.C. Morais (2001) *Magnetic resonance of a dextran-coated magnetic fluid intravenously administered mice* Biophys J **80**: 2483-2486 <sup>8</sup>A.S. Lübbe, C. Bergemann, W. Huhnt, T. Fricke, H. Riess, J.W. Brock and D. Huhn (1997) *Preclinical experiences with magnetic drug targeting: tolerance and efficacy* Cancer Res **57**: 3063-3065 <sup>9</sup>T. Rheinländer, J. Justiz, A. Haller, R. Kötz, W. Weitschies and W. Semmler (1999) *Dynamic properties of fractions yielded by magnetic fractionation of magnetic fluids* IEEE Trans. Magn. **35**: 4055-4057 <sup>10</sup>E.-G. Jäger, K. Schöne and G. Werner (1981) *Lehrwerk Chemie – Arbeitsbuch 5, Elektrolytgleichgewichte und Elektrochemie*, Deutscher Verlag für Grundstoffchemie, p. 266 <sup>11</sup>J. Schmitt, P. Mächtle, D. Eck, H. Möhwald and C.A. Helm (1999) *Preparation and Optical Properties of Colloidal Gold Monolayers* Langmuir **15**: 3256 <sup>12</sup>L. Warzemann, J. Schambach, P. Weber, W. Weitschies, R. Kötz (1999) *LTS SQUID gradiometer system for in vivo magnetorelaxometry* Supercond. Sci. Technol. **12**: 953-955 <sup>13</sup>L. Néel (1955) *Some Theoretical Aspects of Rock-Magnetism* Adv. Phys. **4**, 191-243

**ACKNOWLEDGEMENTS:** This research project is supported by the Deutsche Forschungsgemeinschaft DFG (WE 2555/1) and He 1616/10-1